Constraining the global ocean heat content through the use of CERES derived TOA Energy Imbalance estimates

Andrea Storto[1], Chunxue Yang[1,2], Simona Masina[1,3]

[1]Euro-Mediterranean Center on Climate Change (CMCC), Bologna, Italy

[2]Institute of Atmospheric Science and Climate (ISAC), National Research Council (CNR), Bologna, Italy

[3]National Institute for Geophysics and Volcanology (INGV), Bologna, Italy

Contact: andrea.storto@cmcc.it

Introduction and motivation

Net radiative fluxes at the top of the atmosphere (TOA) balance the absorbed solar minus the outgoing longwave radiations. Greenhouse gases entrapping heat in atmosphere cause global warming of the Earth and lead to long-term positive downward energy imbalance at the top of the atmosphere, emerging from combined observational and modeling studies (e.g. Trenberth et al., 2014, JCLIM). The TOA net radiative flux thus represents a unique diagnostics to monitor the Earth system energy change.

This energy imbalance is mostly absorbed by the global ocean, and is visible in terms of long-term ocean heat content increase. The Argo float observing network has provided since early 2000s an unprecedented sampling of the subsurface temperature, contributing to estimating the percentage of Earth's energy imbalance (EEI) stored in the oceans to be more than 90 % (Riser et al., 2016, NATURE CC), the remaining part being taken by atmosphere, land and cryosphere and being about an order of magnitude smaller than the ocean heat uptake (Trenberth et al., 2016, JCLIM).

Estimates of the Earth's energy imbalance at TOA can be measured by the Clouds and the Earth's Radiant Energy System (CERES, Wielicki et al., 1996, BAMS) instruments on-board the Terra, Aqua and Suomi National Polar-orbiting Partnership (NPP) satellites, combined with other space-borne sensors. Many statistical objective analyses and ocean reanalyses of subsurface temperature fail in capturing the ocean heat content tendencies measured by CERES EBAF data (Smith et al., 2015, GRL; Trenberth et al., 2016, JCLIM).

Variational data assimilation schemes can be derived from the Bayesian analysis equation (e.g. Lorenc, 1986, QJRMS) and offer a straight-forward mathematical framework to ingest observation types with sophisticated observation operators, including for instance CERES derived TOA net radiation fluxes. Aim of this work is to act as a proof-of-concept for constraining ocean heat content tendencies through global TOA energy imbalance data assimilation.

Assimilation of CERES EEI

The Ocean reanalysis system is a coarse resolution configuration of C-GLORS (ORCA2 with 31 vertical levels and partial steps), with 3DVAR/FGAT assimilation of in-situ profiles from U.K. MetOffice EN4 (Good et al., 2013, JGR-O).

In order to assimilate EEI estimates in the 3DVAR, the variational cost function is modified as follows (to render explicit the new penalty term that involves the assimilates CERES data):

$$J(\boldsymbol{\delta x}) = \boldsymbol{\delta x}^{\mathrm{T}}\, \boldsymbol{B}^{-1}\, \boldsymbol{\delta x} + (\boldsymbol{H\delta x} - \boldsymbol{d})^{\mathrm{T}} \boldsymbol{R}^{-1} (\boldsymbol{H\delta x} - \boldsymbol{d}) + (\delta EEI - d^{EEI})^{\mathrm{T}} R_{EEI}^{-1} (\delta EEI - d^{EEI})$$

δEEI is the increment of δx in TOA net radiation space, and d^{EEI} is the misfit between CERES EBAF-TOA observation and the background-equivalent, respectively given by:

$$\delta EEI = f(\boldsymbol{\delta x}) = \frac{\rho\, c_p}{\Delta t} \int_V [\boldsymbol{\delta T}]\, dV$$

$$d^{EEI} = OHCT_{EBAF} - OHCT_b = \beta\, y_{EBAF} - f(\boldsymbol{x_b}) = \beta\, y_{EBAF} - \frac{\rho\, c_p}{\Delta t} \int_V [\boldsymbol{T_{t2}^b} - \boldsymbol{T_{t1}^b}]\, dV$$

$OHCT_{EBAF}$ is the CERES derived observations of global ocean heat content tendency, equal in turn to CERES EBAF TOA (Ed4) global monthly mean net radiation multiplied by the coefficient β (0.93) that determines the ratio of EEI absorbed by the global ocean.

$\boldsymbol{T_{t1}}^b$ and $\boldsymbol{T_{t1}}^b$ are background temperature at the beginning (t1) and end (t2) of the assimilation time-window; $\boldsymbol{\delta T}$ is the temperature increment. Extension of this scheme for 4DVAR is straight-forward.

R_{EEI} is the error associated to the EEI observations, quantified in 0.4 W m^{-2} as the approximate squared sum of the variances of representation error (0.3 W m^{-2}, corresponding to the EEI monthly global anomaly for non-ocean components) and instrumental error (assumed equal to 0.3 W m^{-2}, estimated by Loeb et al. (2016, RS) as standard deviation of the differences of CERES measurements from different satellite platforms).

Results: impact of the assimilation

***Experiments**: C-GLORSv5: reference CMCC eddy-permitting reanalysis; INS: Assimilation of in-situ profiles only; INS&OHCT: Assimilation of in-situ profiles and CERES EEI data; NOASS: control experiment without data assimilation: OHCT: assimilation of CERES EEI data only*

Heat Content Tendency (W m-2)	CERES EBAF Ed4	C-GLORS v5	INS	INS&OHCT	NOASS	OHCT
Mean	0.67	0.67	0.38	0.67	2.12	1.00
Correlation (monthly means)	-	0.84	0.80	0.89	0.87	0.88
Correlation (monthly means with seasonal cycle removed)	-	0.06	0.14	0.51	0.80	0.82
Standard Deviation (monthly means)	6.58	9.44	15.91	6.90	10.3	5.94
Standard Deviation (monthly means with seasonal cycle removed)	0.55	1.01	0.90	0.74	0.75	0.46
Seasonal Amplitude	8.41	10.91	12.12	7.04	13.09	6.79
SLA RMSE (cm)	-	6.78	7.28	7.30	8.14	8.06
SST RMSE (°C)	-	0.30	0.69	0.69	0.78	0.78
T 0-100 RMSE (°C)	-	1.06	1.35	1.34	1.87	1.85
T 100-300 RMSE (°C)	-	0.87	1.20	1.20	1.66	1.65
T 300-800 RMSE (°C)	-	0.62	0.80	0.80	1.11	1.10
S 0-100 RMSE (psu)	-	0.34	0.39	0.39	0.64	0.65
S 100-300 RMSE (psu)	-	0.15	0.20	0.20	0.33	0.32
S 300-800 RMSE (psu)	-	0.07	0.08	0.08	0.13	0.13

Table: Mean, standard deviation, seasonal amplitude and correlation with respect to CERES EBAF Ed4 data of the four experiments presented in the text, along with C-GLORS v5, relative to the 2001-2013 period. The seasonal amplitude is calculated fitting the time-series to a sinusoidal function. The correlation is significant if greater to 0.20 (at 99% confidence interval). In the bottom part of the Table, skill scores are reported for the four experiments, along with C-GLORS, for the period 2001-2013. SLA root mean square errors (RMSE) are calculated against gridded altimetry data from CMEMS (AVISO), SST RMSE against NOAA SST OIv2 analyses, while temperature (T) and salinity (S) RMSE against all available observations extracted from the UKMO EN4 dataset, before their eventual assimilation.

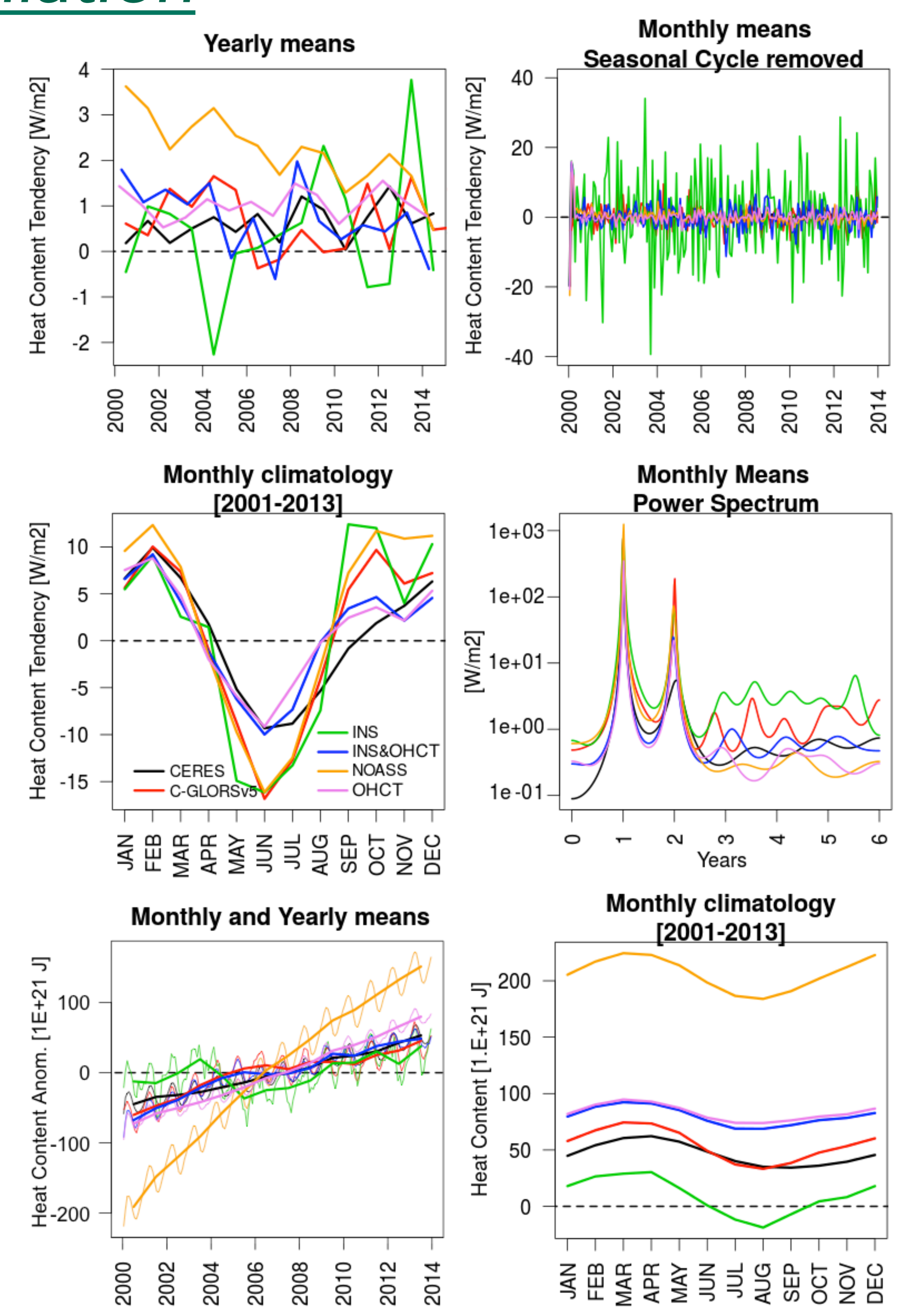

Figure: Results from the experiments presented in the text. Top left and right panels: heat content tendency as yearly means and monthly means (with seasonal cycle removed), respectively. Middle left panel: monthly climatology (2001-2013) of the heat content tendency; middle right panel: power spectrum of the heat content tendency. Bottom panels: heat content anomaly monthly and yearly means (left) and monthly climatology (2001-2013, right)

Heat Content: Horizontal and vertical Trends

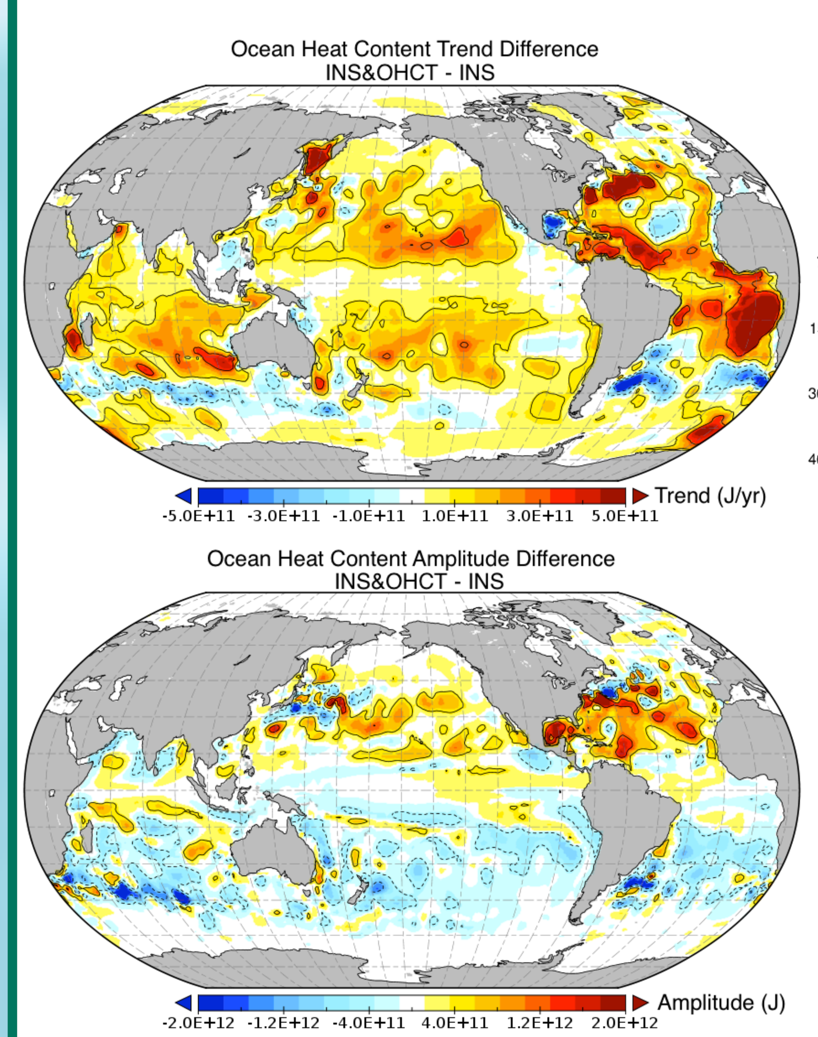

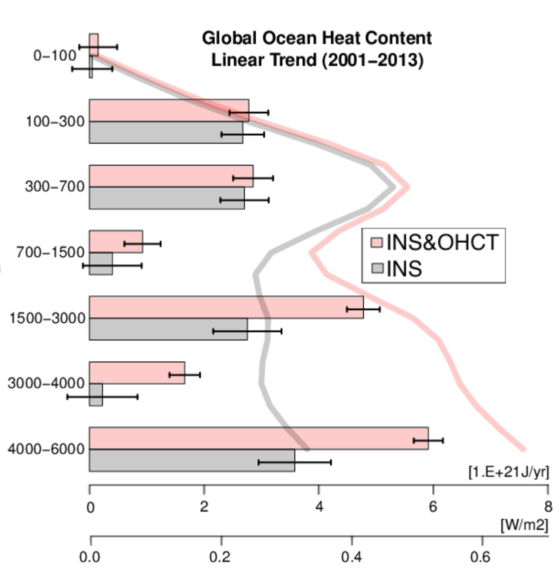

***Left:** Total column ocean heat content trend (top left panel) and seasonal amplitude (bottom left panel) differences for INS&OHCT minus INS (right panels).*

***Right:** Global ocean heat content trend for different vertical regions (bars) and integrated from the sea surface (lines) for INS&OHCT (light red) and INS (gray).*

Most of warming difference is found in the Atlantic Ocean and, to a lesser extent, in the Pacific Ocean mid-latitudes and eastern Indian Ocean. This distribution is linked to both the background-error covariances and the geographical sampling of in-situ.

The seasonal amplitude map difference suggests that the decrease in the Southern Hemisphere leads to the globally averaged decrease. The Northern Hemisphere on the contrary is characterized by an increase of amplitude in the Atlantic sector, while the Pacific sector exhibits a decrease and an increase in the western and eastern regions, respectively.

The sketch of the right panel indicates that most of CERES data induced warming occurs below 1500 m, consistently with the fact that in-situ profiles well constrain the upper ocean, and with the common speculation that the missing energy seen by CERES but not by most ocean heat content estimates during the hiatus period stems from the unmeasured deep ocean warming.

Propagation of EEI increments

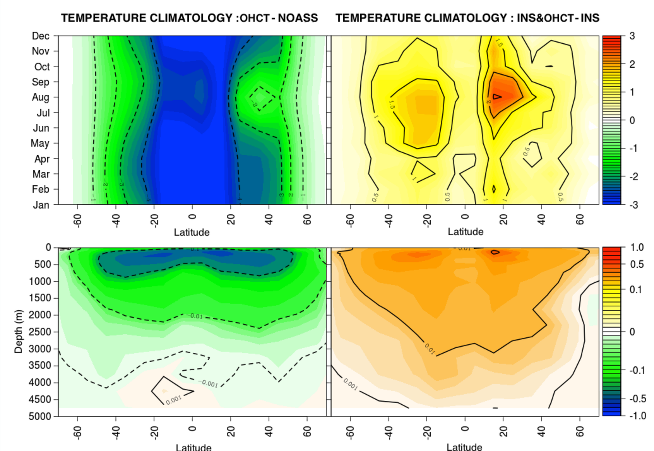

Figure: Temperature climatology difference as a function of latitude and month of the year (top panels) and latitude and depth (bottom panels), for OHCT minus NOASS (left panels) and INS&OHCT minus INS (right panels). The scale for the bottom panel is logarithmic.

When CERES data are assimilated, the temperature increase peaks in July and August (for both hemispheres, at around 20S and 20N). The warming also peaks in the subtropics and at around 200 m of depth, with the Southern Ocean having a slightly deeper penetration of the warming, in accordance with recent findings (Stephens and L'Ecuyer, 2015, ATMRES).

Key points

- *Ocean reanalyses show global heat content tendencies whose variability barely matches that from radiation imbalance measurements at the TOA*
- *A scheme is introduced to assimilate energy imbalance estimates into ocean reanalyses for constraining the global heat budget*
- *The new assimilation successfully corrects the heat content tendency variability without any loss of accuracy in the reanalysis, limiting the occurrence of the warming hiatus, in accordance with CERES data*
- *The EEI assimilation scheme can be extended to Earth System reanalyses or climate simulations to constrain the global energy budget*

This work is published in: Storto, A., C. Yang, and S. Masina (2017), Constraining the Global Ocean Heat Content Through Assimilation of CERES derived TOA Energy Imbalance Estimates, *Geophys. Res. Lett.*, Accepted for publication (In Press).

Acknowledgements: *This study was supported by the CMEMS and the FP7 ERA-CLIM2 project.*